Geophys. J. Int. (1999) **136,** 567–585

New extended thin-sheet approximation for geodynamic applications—I. Model formulation

Sergei E. Medvedev[1,*] and Yuri Yu. Podladchikov[2]

[1] *Institute of Earth Sciences, Uppsala University, Vilavagen* 16, SE-752 36 *Uppsala, Sweden.*
[2] *Geologisches Institut, ETH-Zurich, Sonneggstrasse* 5, CH 8092, *Zurich, Switzerland*

Accepted 1998 September 23. Received 1998 September 16; in original form 1998 February 13

SUMMARY

Thin-sheet approximations are widely used in geodynamics because of their potential for fast computation of 3-D lithospheric deformations using simple numerical techniques. However, this simplicity imposes limits to boundary conditions, rheological settings and accuracy of results. This paper presents a new approach to reduce these restrictions. The mathematical formulation of the model involves the construction of the depth distributions of stress and velocity fields using asymptotic approximations of 3-D force balance and rheological relations. The asymptotic treatment is performed on the basis of a small geometry parameter ε (thickness to width ratio of the thin sheet) with a high accuracy while keeping terms which are capable of generating strong singularities due to possible large variations in material properties in layered systems. The depth profiles are verified by a condition of exact equilibrium in the depth-integrated force balance and by an asymptotic approach to the boundary conditions. The set of analytical depth profiles of velocities and stresses, together with the 2-D equations representing the integrated force balance, result in an extended thin-sheet approximation (ETSA). The potential of the ETSA is demonstrated by applications to problems with different types of boundary conditions and consideration of the types of systems of equations governing each case. These studies have not found any strong limitations to the boundary conditions considered and demonstrate the greater generality and higher accuracy of ETSA in comparison with the previous generation of thin-sheet approximations. The accompanying paper demonstrates the results of 2-D experiments based on ETSA.

Key words: creep, lithospheric deformation, numerical techniques, perturbation methods, shear stress.

1 INTRODUCTION

3-D modelling is one of the most important problems in geodynamics. However, direct 3-D numerical investigations are extremely complex and highly expensive (Braun 1993; Braun & Beaumont 1995). To resolve this problem, additional analytical investigations are being considered based on the specific properties of particular geological settings.

Problems in geodynamics are often characterized by geometrical singularity when the horizontal scale is much larger than the vertical scale (so-called 'thin-sheet' structures). Scales can range from salt domes ($\sim$5 km in horizontal scale) to continent–continent collisions. Thin-sheet approximations attempt to estimate the depth dependence of the thin sheet analytically and reduce the originally 3-D (2-D) system to a set of 2-D (1-D) equations for numerical calculation.

The numerical advantages of the thin-sheet approximation are obvious. The solution of 2-D equations (as opposed to 3-D equations) can be performed on smaller computers or with higher accuracy using well-known simple numerical techniques. However, the analytical support of existing approaches is simplified mainly by neglecting some of the terms in the full governing equations. This inevitably restricts the applications of existing thin-sheet approaches.

* Present address: Department of Oceanography, Dalhousie University, Halifax, NS, Canada, B3H 4J1. E-mail: sergei@adder.ocean.dal.ca

Three types of thin-sheet approximations are in current use in geodynamic models. One assumes a negligible vertical gradient of horizontal velocity (hereafter the 'PS' or 'pure shear' approach). The second involves gravitational spreading defined by the equilibration of vertical gradients of horizontal velocities (hereafter the 'SS' or 'simple shear' approach). The third recognizes the importance of the long-term flexural rigidity of the lithosphere by ensuring equilibrium in bending moments (hereafter the 'FP' or 'flexing plate' approach). The differences between these approaches are defined by the boundary conditions applied in each case (Fig. 1). The suggested abbreviations do not assume a complete explanation of the physics behind the approximations, but are used to distinguish between different models.

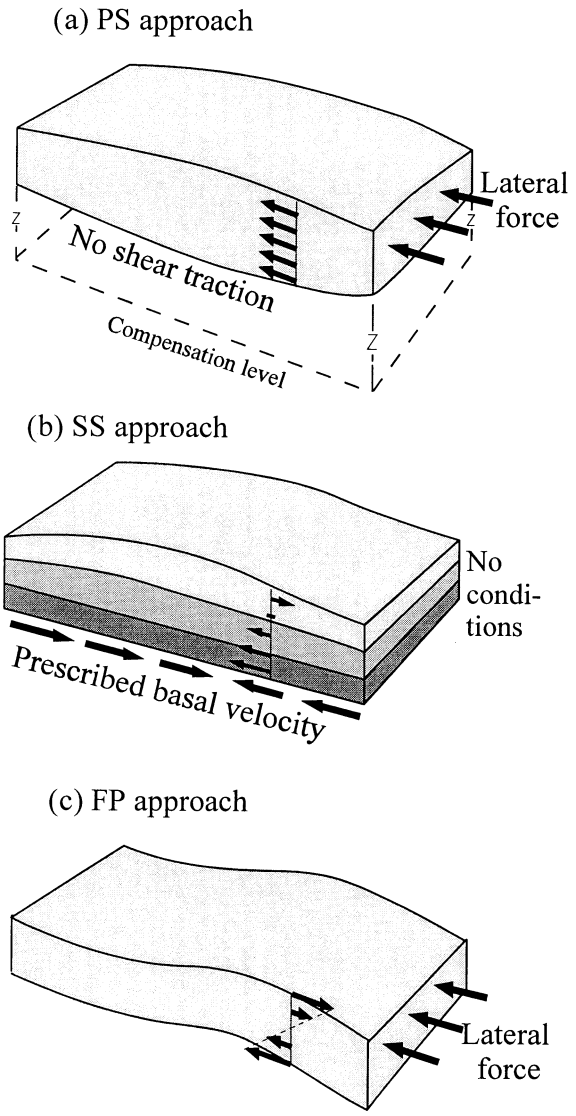

Figure 1. Three types of thin-sheet approximations are used in geodynamics. These types are determined by the horizontal boundary conditions applied and the rheological profiles possible. (a) The PS approach is characterized by dynamic boundary conditions (normal stresses). Creep rheology is averaged through a model depth. (b) The SS approach is characterized by a kinematic boundary condition(s) with the prescription of the velocity on an external boundary(ies). Layered structures can be investigated on the basis of creep rheology. (c) The FP approach is characterized by the flexural rigidity of a strong layer (plate). The lateral force results in bending moments. When an elastic rheology is used, shear traction and normal stress can be set on external boundaries. If a strong layer creeps, the boundary conditions are similar to case (a) without shear stresses on external boundaries. The velocity profiles possible are demonstrated on the front of each slab.

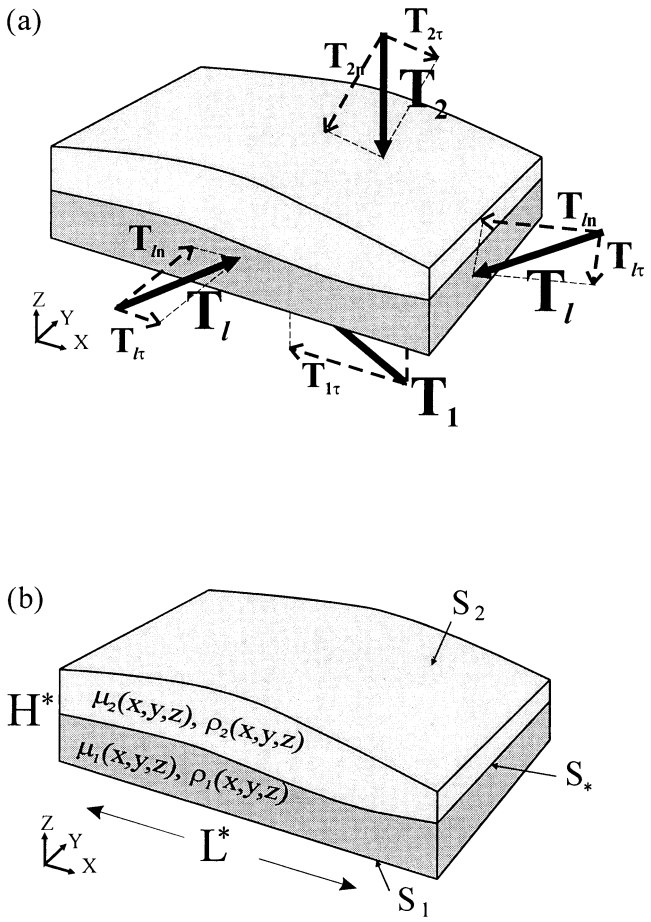

Figure 2. A general view of a thin sheet. (a) Generalized forces can be specified as either external forces (stresses) or velocities (strain rates) or combinations of the two. Note that external generalized forces can have normal and tangential components at any boundary. (b) The 3-D geometric settings illustrate the definition of a thin sheet by condition $L^* \gg h^*$. Layered systems can be investigated by introducing an internal rheological boundary S_*. Note that all boundaries can be material or non-material. S_1 can thus be a non-material level of compensation which does not move with the surrounding material.

Artyushkov (1973, 1974) investigated forces in a thin sheet under PS-type boundary conditions. On the basis of advanced force balance (including equilibrium of moments), he investigated possible distributions of forces and velocities with respect to depth and time. The estimates of relaxation times of depth variations presented in these works can be considered as the theoretical basis of the PS approach.

England & McKenzie (1982, 1983) introduced the term 'thin-sheet approximation' while investigating an isostatic system driven from the lateral boundaries with a stress-free upper surface and no shear traction on the bottom boundary (Fig. 1a). They used a power-law creep averaged over the depth to model the rheology of a thin sheet. The vertical gradient of horizontal velocities can be neglected if the system is underlain by an inviscid substratum. This approach has been further developed by additional analytical investigations (England 1983; England *et al.* 1985; Sonder & England 1986; Jones *et al.* 1996). Several geodynamic applications are illustrated in Table 1 of Ellis *et al.* (1995).

The advantage of the PS approach is that a wide range of intercontinental collisions can be modelled by driving a stiff indentor of any shape into a thin lithospheric sheet at any velocity (Vilotte *et al.* 1982; Vilotte *et al.* 1986; England & Houseman 1986; Houseman & England 1986, 1993; Sonder *et al.* 1986). This model allows simple descriptions of a number of active tectonic zones (England & Jackson 1989). Among the recent applications of the PS approach for the modelling of specific regional deformations is the work of Sobouti & Arkani-Hamed (1996).

The most significant limitation of the PS approach is that it is unable to satisfy a variety of horizontal boundary conditions. Neglecting depth variations of velocity does not allow the generation of local instabilities leading to folding, pinching, etc. However, a large difference in mechanical strength between a shortening thin sheet and its surroundings is known to result in folding (Ramberg 1970a,b; Smith 1975; Turcotte & Schubert 1982). The PS approach assumes an average rheology throughout the depth of the thin sheet, which means that it cannot be applied to problems involving significant layering of the lithosphere.

The SS approach was developed by several authors in several works. The governing equations of this approach are similar to the theory of a lubricating layer (Schlichting 1968). The method is fully described in the works of Zanemonetz *et al.* (1974, 1976) and Lobkovsky & Kerchman (1991). A prescribed basal velocity field leads to spreading controlled by the equilibration of gravity with the vertical gradient of horizontal velocity within the layer (Fig. 1b), which is described by different forms of creep rheology. The SS approach is also in wide use: it has been applied to the spreading of lava (Huppert 1982; Huppert *et al.* 1982; Miyamoto & Sasaki 1997), the evolution of salt domes (Talbot *et al.* 1998), lithosphere contractions (Lobkovsky & Kerchman 1991; Buck & Sokoutis 1994) and investigating the shapes of domes on Venus (McKenzie *et al.* 1992). Bird (1991), Buck (1991) and Kaufman & Royden (1994) used this approach to investigate the flow of the lower crust during deformation of the lithosphere.

The advantage of the SS model is its ability to satisfy a variety of horizontal boundary conditions such as in investigations of two-layer lithospheric systems (Zanemonetz *et al.* 1974, 1976). Deformation of a layered lithosphere caused by movements in the mantle has been investigated by Myasnikov *et al.* (1993) and Mikhailov *et al.* (1996). Medvedev (1993) applied the SS approach to the modelling of multilayered subhorizontal structures, which he based on analytical investigations of Svalova (personal communication, 1988). However, the assumption of a velocity field of the same order across a model domain does not allow large viscosity contrasts between the layers. The latest theoretical development of Royden (1996) partly resolved this problem and demonstrated the great potential of the SS approach for the modelling of strongly layered orogenic systems.

Westaway (1993), Ribe (1996) and Sleep (1996, 1997) developed a variation of the SS approach to investigate the case where both the upper and lower external horizontal boundaries are subjected to prescribed velocities to explore the interior flow field of a hot mantle plume.

The main restriction of the SS approach is that lateral boundary conditions are only passive and cannot be driven.

Several attempts to combine the PS and SS approaches have been successful. Ellis *et al.* (1995) investigated the coupling of two layers using a combination of SS and PS approaches. They developed an advanced system of equations to describe the flow in a two-layer system with highly uneven viscosity. Bird (1989) investigated a two-layer system using the PS approach to describe each layer; layer interaction was modelled using the SS approach. Even though some of the limitations of the thin-sheet approximation remained, Bird's model is particularly suited to the numerical finite element technique and has great potential for modelling global structures with complex rheology (e.g. Bird & Kong 1994).

The problems of the interaction of two or more rheological layers is poorly described by the first two types of thin-sheet models. This is because the PS and SS approaches cannot handle characteristic wavelengths even if the contrast in (effective) viscosity is high and the dominant wavelengths are much longer than the thickness of the layers. All existing thin-sheet approaches became ill-conditioned if the model involves a density inversion, and numerical modelling cannot be based on these equations. The mathematical difficulties are similar to those that arise when attempting to solve the heat conduction equation backwards in time.

From a mathematical point of view, the PS and SS types of thin-sheet approximations lose the generality by neglecting terms from the governing equations. External tractions cannot be applied to horizontal boundaries using the PS approach because it omits all terms explaining the stress distribution with depth. External lateral stresses cannot be investigated by the SS approach because it neglects all horizontal stress derivatives.

The FP approach was developed mostly on the basis of the thin elastic plate theory presented by Timoshenko & Woinowsky-Krieger (1959). According to this theory, a lateral force applied to a pre-deformed plate gives rise to moments which cause additional flexural bending (Fig. 1c). This redistributes horizontal stresses and explains geophysical observations in areas

where the local compensation model (Airy isostasy) breaks down. Such mechanisms were introduced by applying elastic rheology to lithospheric processes (e.g. Dubois *et al.* 1977; Karner & Watts 1983; Lyon-Caen & Molnar 1983). However, pure elastic models of the lithosphere failed to explain some theoretical and geophysical observations (McNutt *et al.* 1988; Burov & Diament 1992, 1995). Multilayered lithospheric structures were investigated on the basis of the FP approach to resolve these problems (McNutt *et al.* 1988; Ranalli 1994). Extensions of the FP approach were developed by Burov & Diament (1992, 1995), Aouvac & Burov (1996) and Cloetingh & Burov (1996) by introducing weak layers governed by the SS creep approach. This allows the application of more realistic strength profiles for the lithosphere. Depending on crustal thickness, temperature conditions and upper-surface processes, flexural decoupling between strong layers can occur in these models, which can explain a variety of lithospheric phenomena.

One of the advantages of the FP approach is that it can describe the folding of rocks because of its ability to take account of different characteristic behaviours for each layer. This property distinguishes the FP approach from the PS and SS approaches.

Although many natural folded layers exhibit elastic (or plastic) behaviour, there are other layered structures which demonstrate viscous (creep) behaviour. Application of the FP approach to the description of pure creep in layered structures with uneven viscosity distributions is known as the Biot theory of folding (after Turcotte & Schubert 1982; Biot 1961; Ramberg 1970a,b; Fletcher 1977). This theory is based on a thin-sheet approximation of the equilibrium of bending moments in thin viscous plates. Turcotte & Schubert (1982, eq. 6-181) derived the 'general equation for the bending of a thin viscous plate' using the clear similarity between viscous and elastic forces and moments (see also Ramberg 1970a; De Bremaecker 1977). This equation describes how the evolving vertical displacement is controlled by the distribution of normal external forces.

Application of this is limited to cases with strong viscosity contrasts because it neglects the external shear forces imposed by any surroundings with low viscosity.

The limitations of existing models are not a necessary feature of thin-sheet approaches. The extended thin-sheet approximation (ETSA) developed here is based not on a simplification but on asymptotic investigations of the balance of forces. The 3-D deformation is driven by external forces (acting on all boundaries) and controlled by rheological properties within those boundaries. The dynamic (tractions) or kinematic boundary forces (boundary velocities), or their combination at both lateral and horizontal boundaries, can be specified in the ETSA (Fig. 2a). Geometrical settings are required to satisfy the scaling assumption, $\varepsilon = H^*/L^* \ll 1$, in the definition of a thin-sheet approximation (Fig. 2b). Due to the long-term effect of gravity and lateral heat conduction, the lithosphere is usually subhorizontally mechanically layered, so this assumption is easily acceptable for geodynamic modelling. Certainly, horizontal multilayers are a common configuration at the onset of many new tectonic processes.

The model is formulated in two parts. The first part investigates the mass and force balance of a thin sheet, independent of its rheology. The second part employs a creep rheology to close the system of equations. The new approach is illustrated by its application to various types of boundary conditions to present the governing systems of equations for each case.

This paper is the first work in a sequence of developments and applications of the new extended thin-sheet approach. The accompanying paper demonstrates the results of 2-D experiments on the basis of ETSA (Medvedev & Podladchikov 1999). 3-D tests are in preparation.

2 FORMULATION INDEPENDENT OF RHEOLOGY

Rheologically independent relationships are derived in this section, which assumes stress (force) and mass balance in continuous media.

To emphasize the difference between coordinates we distinguish vertical and horizontal characteristic length scales in dimensional analysis (Tables 1 and 2). Scaling assumptions introduced in Table 2 include the also inequality of scales for different components of the stress tensor. This method of scaling results in the appearance of a small parameter ε in the equations (Zanemonetz *et al.* 1974, 1976; Fowler 1993; Medvedev 1993). The symmetry of two horizontal coordinates (x and y) is emphasized by using indexed abbreviations in equations (x_i, Table 3). Projections of 3-D equations onto two horizontal axes give the same results, and indexed presentation of these projections allows avoiding the repetitions [e.g. eq. (5) represents two projections of the force balance which are equal up to substitutions $x \leftrightarrow y$ and therefore horizontal coordinates are denoted by indexed x]. The indexed abbreviation also allows the use of the summation convention (e.g. eq. 1). The vertical coordinate differs significantly and is therefore not abbreviated.

2.1 Kinematics

A set of kinematic relationships describing the motions of boundaries while maintaining mass balance is independent of rheology. The mass balance for incompressible media is

$$\frac{\partial v_j}{\partial x_j} + \frac{\partial v_z}{\partial z} = 0 . \tag{1}$$

Note that we use abbreviations for horizontal coordinates and summation convention (Table 3). For the change in vertical velocity

Table 1. Definition of widely used dimensionless variables[†].

Variable	Definition	Coordinate dependence	Dimensional scale
a_z	Vertical boundary conditions partitioning coefficient (eq. 30)	–	–
D, E, F, G, J, $\underline{Q}$	Coefficients for evaluation of horizontally oriented stress tensor components τ_{xx}, τ_{xy}, τ_{yy} (eqs 43, 44)	(x, y, z)	–
$M_\rho = \overline{z_c \rho}$	Density momentum in vertical force balance (eqs 25)	(x, y)	$\rho^*(H^*)^2$
P	Isotropic part of stress tensor with minus sign ('pressure' in the text)	(x, y, z)	P^*
R_x, R_y, R_z	Dynamic integration functions (eqs 18, 14)	(x, y)	$P^* \cdot \varepsilon$, $P^* \cdot \varepsilon$, P^*
S_1, S_2	Lower and upper boundaries of the system	(x, y)	H^*
$(T_x, T_y, T_z)\|_{S_m}$	Vectors of boundary tractions on the external surface S_m	(x, y)	$(P^* \cdot \varepsilon, P^* \cdot \varepsilon, P^*)$
t	Time	–	t^*
(V_x, V_y, V_z)	Basal velocity vector (eq. 35), kinematic integration functions	(x, y)	(V_x^*, V_x^*, V_z^*)
(v_x, v_y, v_z)	Velocity vector	(x, y, z)	(V_x^*, V_x^*, V_z^*)
w, z_c	Reference surface and centred z coordinate during integration of vertical force balance (eq. 12)	(x, y)	H^*
(x, y, z)	Coordinate system (capital letters denote directions and Z-axis is directed upwards)	–	(L^*, L^*, H^*)
τ	Deviatoric part of stress tensor ('stress tensor' in text); see scaling for its components below	(x, y, z)	–
τ_{ij}, τ_{zz}	Horizontal and vertical components of stress tensor	(x, y, z)	P^*
τ_{xz}, τ_{yz}	Vertical shear stresses	(x, y, z)	$P^* \cdot \varepsilon$

[†] Non-dimensional variables are used without special notations.

Table 2. Characteristic values.

Value	Definition	Units	Comments
H^*	Vertical length scale	m	
L^*	Horizontal length scale	m	
g	Acceleration due to gravity	m s^{-2}	
P^*	Stress	Pa	$P^* = \rho^* g H^*$
t^*	Time	s	$t^* = L^*/V_x^* = H^*/V_z^*$
V_x^*	Horizontal velocity	m s^{-1}	$V_x^* = P^* L^*/\mu^*$
V_z^*	Vertical velocity	m s^{-1}	$V_z^* = P^* H^*/\mu^* = \varepsilon V_x^*$
ε	Small geometry parameter	–	$\varepsilon = H^*/L^* \ll 1$
μ^*	Viscosity	Pa s	
ρ^*	Density	kg m^{-3}	

Table 3. Designation.

Attribute	Definition	Examples
	Superscripts	
'prime'	Approximate values of stress functions (eqs 13, 17)	
*	Characteristic value (Table 1)	
d	Dimensional value	Using Table 1, for any function $F^d = F \cdot$(Dim.scale)
	Subscripts	
i, j, k	Abbreviated indices related to horizontal coordinates (x, y). i usually refers to equation orientation, while j, k usually assume summation	$V_i \leftrightarrow \{V_x, V_y\}$, $\frac{\partial \tau_{ij}}{\partial x_j} \leftrightarrow \left\{ \frac{\partial \tau_{xx}}{\partial x} + \frac{\partial \tau_{xy}}{\partial y} \frac{\partial \tau_{yx}}{\partial x} + \frac{\partial \tau_{yy}}{\partial y} \right\}$
*	Skipping the differential operator in coefficients (44) (see notes after equation)	
	Special designation	
Vertical bar with one subscript	Function value on selected z level	$v\|_{S_1} = v(x, y, S_1(x, y))$
Vertical bar with two limits	Difference operator between its upper and lower limits	$(z_c \cdot \tau_{iz})\|_{S_1}^{S_2} = (S_2 - w)\tau_{iz}\|_{S_2} - (S_1 - w)\tau_{iz}\|_{S_1}$
Overbar (1)	For continuous functions: z integrating through the system (note that there is no normalizing by H)	$\overline{P}(x, y) = \int_{S_1}^{S_2} P(x, y, z) dz$, $\overline{z \cdot \rho} = \int_{S_1}^{S_2} z \cdot \left(\int_{S_1}^{z} \rho \, dz' \right) dz$
Overbar (2)	For discrete functions: sum of values of the function at upper and lower external boundaries	$\overline{T_i} = T_i\|_{S_1} + T_i\|_{S_2}$, $\overline{z \cdot T_i} = S_1 T_i\|_{S_1} + S_2 T_i\|_{S_2}$
Repeated indices in equations	The Einstein summation convention: implication of a sum for all combinations in respect of x and y	$\tau_{ii} = \sum_i \tau_{ii} = \tau_{xx} + \tau_{yy}$, $\frac{\partial \tau_{ij}}{\partial x_j} = \frac{\partial \tau_{ix}}{\partial x} + \frac{\partial \tau_{iy}}{\partial y}$, $\frac{\partial^2 \tau_{ij}}{\partial x_k^2} = \frac{\partial^2 \tau_{ij}}{\partial x_k \partial x_k} = \frac{\partial^2 \tau_{ij}}{\partial x^2} + \frac{\partial^2 \tau_{ij}}{\partial y^2}$

across any material or non-material interfaces S_m and S_l, mass conservation in integrated form is

$$\int_{S_l}^{S_m} \frac{\partial v_j}{\partial x_j}\, dz + v_z|_{S_m}^{S_l} = 0\,. \tag{2}$$

For any material interface S_m, the impenetrability condition gives (Zanemonetz *et al.* 1974)

$$\frac{\partial S_m}{\partial t} + v_j|_{S_m} \frac{\partial S_m}{\partial x_j} = v_z|_{S_m}\,. \tag{3}$$

For the distance between any material interfaces S_m and S_l, combining eq. (3) and mass conservation (eq. 2) gives

$$\frac{\partial (S_m - S_l)}{\partial t} + \frac{\partial}{\partial x_j}\left(\int_{S_l}^{S_m} v_j\, dz\right) = 0\,. \tag{4}$$

2.2 3-D force balance

The dimensionless force balance equations in terms of stresses are (Turcotte & Schubert 1982)

$$-\frac{\partial P}{\partial x_i} + \frac{\partial \tau_{ij}}{\partial x_j} + \frac{\partial \tau_{iz}}{\partial z} = 0\,, \tag{5}$$

$$\varepsilon^2 \frac{\partial \tau_{jz}}{\partial x_j} + \frac{\partial (\tau_{zz} - P)}{\partial z} = \rho\,. \tag{6}$$

Note that eq. (5) represents two horizontal projections of the force balance using abbreviation convention (Table 2). The small parameter ε arises in the vertical projection of the force balance (eq. 6) due to different scalings of different components of the deviatoric part of the stress tensor τ and due to different coordinate scalings (see Table 1). Integration with depth results in

$$-\frac{\partial \overline{P}}{\partial x_i} + \frac{\partial\, \overline{\tau_{ij}}}{\partial x_j} + \overline{T_i} = 0\,, \tag{7}$$

$$\varepsilon^2 \frac{\partial\, \overline{\tau_{jz}}}{\partial x_j} + \overline{T_z} = \overline{\rho}\,. \tag{8}$$

The transformation of eqs (5) and (6) to integrated eqs (7) and (8) is performed by integration and the changing of integration–differentiation order. Vectors of boundary traction at the upper surface ($m=2$) and the base ($m=1$) are ($T_x|_{S_m}$, $T_y|_{S_m}$, $T_z|_{S_m}$), and these are related to the internal stresses by

$$T|_{S_m} = -\tau \cdot n_m + P n_m\,, \tag{9}$$

where n_m is a unit external vector normal to S_m. Projected onto the horizontal and vertical axes,

$$\begin{aligned} T_i|_{S_m} \cdot (-1)^m &= \left(P \frac{\partial S_m}{\partial x_i} + \tau_{ij} \frac{\partial S_m}{\partial x_j} + \tau_{iz}\right) \Big/ a_m\,, \\ T_z|_{S_m} \cdot (-1)^m &= \left(-\varepsilon^2 \tau_{jz} \frac{\partial S_m}{\partial x_j} + \tau_{zz} - P\right) \Big/ a_m\,, \end{aligned} \tag{10}$$

where $(-1)^m$ is due to opposite orientations of normal vectors on the top and bottom of the thin sheet and

$$a_m = \sqrt{1 + \left(\varepsilon \frac{\partial S_m}{\partial x}\right)^2 + \left(\varepsilon \frac{\partial S_m}{\partial y}\right)^2} \approx \left(1 - \frac{1}{2}\left(\varepsilon \frac{\partial S_m}{\partial x}\right)^2 - \frac{1}{2}\left(\varepsilon \frac{\partial S_m}{\partial y}\right)^2\right)^{-1} \approx 1 \tag{11}$$

is the correction of the length of the normal vector applied to the right-hand sides of eqs (10) as required for the normal vector to be unity in eq. (9). The small correction ($\sim \varepsilon^2$) is neglected in the developments that follow.

The averages of the shear stresses on vertical planes (τ_{xz} and τ_{yz}) can be expressed via moments of the stresses in the horizontal plane (τ_{xx}, τ_{yx}, τ_{yy}) and pressure. Integration by parts gives

$$\begin{aligned} \overline{\tau_{iz}} &= \int_{S_1}^{S_2} \tau_{iz}\, dz = (z_c \cdot \tau_{iz})|_{S_1}^{S_2} - \int_{S_1}^{S_2} z_c \cdot \frac{\partial \tau_{iz}}{\partial z}\, dz = (z_c \cdot \tau_{iz})|_{S_1}^{S_2} + \int_{S_1}^{S_2} z_c \cdot \left(-\frac{\partial P}{\partial x_i} + \frac{\partial \tau_{ij}}{\partial x_j}\right) dz \\ &= \overline{z_c}\, \overline{T_j} + \left[\frac{\partial\, \overline{z_c \cdot \tau_{ij}}}{\partial x_j} - \frac{\partial \overline{z_c \cdot P}}{\partial x_i} + \overline{\tau_{ij}} \frac{\partial w}{\partial x_j} - \overline{P} \frac{\partial w}{\partial x_i}\right], \end{aligned} \tag{12}$$

where $z_c = (z - w)$ is the centered z coordinate and $w(x, y)$ is the reference surface for the calculation of moments; $\overline{(z_c T_i)}$, $\overline{z_c \cdot P}$ and $\overline{z_c \cdot \tau_{ij}}$ are moments of T_i, P and τ_{ij} respectively. It can be shown that the results do not depend on the position of the reference surface. However, being able to change the position of the reference surface introduces an extra degree of freedom into the ETSA; possible specifications are discussed in Section 5.

2.3 Depth profiles of pressure and vertical shear stresses

Integration of eq. (6) yields

$$P(x, y, z) = -\ R_z - \tau_{jj} - \int_{S_1}^{z} \rho dz' + \varepsilon^2 \int_{S_1}^{z} \frac{\partial \tau_{iz}}{\partial x_i}\, dz' \cong -\ R_z - \tau_{jj} - \int_{S_1}^{z} \rho dz' = P', \tag{13}$$

where R_z is a new dynamic integration function,

$$R_z(x, y) = (\tau_{zz} - P)|_{S_1}\,. \tag{14}$$

The definition of the deviatoric part of the tensors used in the transformation of eq. (6) to (13) is

$$\tau_{jj} + \tau_{zz} = 0\,. \tag{15}$$

The profile $P'(x, y, z)$ in (13) represents asymptotic approximation to the accurate profile P while neglecting the term with small parameter ε. The change of the inexact normal vertical stresses across the layer is equal to lithostatic pressure at the bottom of the thin sheet (from eq. 13):

$$(-P' + \tau_{zz})|_{S_2} - (-P' + \tau_{zz})|_{S_1} = \overline{\rho}\,. \tag{16}$$

Integration of eq. (5) and substitution of the approximation of P from (13) yields

$$\begin{aligned}\tau_{iz}(x, y, z) &= R_i + \int_{S_1}^{z} \left(\frac{\partial P}{\partial x_i} - \frac{\partial \tau_{ij}}{\partial x_j} \right) dz' \\ &\cong R_i - \frac{\partial R_z}{\partial x_i}\,(z - S_1) - \int_{S_1}^{z} \left(\frac{\partial \tau_{jj}}{\partial x_i} + \frac{\partial}{\partial x_i} \int_{S_1}^{z'} \rho dz'' + \frac{\partial \tau_{ij}}{\partial x_j} \right) dz' = \tau'_{iz}\,.\end{aligned} \tag{17}$$

This expression gives an asymptotic approximation, τ'_{iz}, to the vertical shear stress, τ_{iz}, neglecting all terms with ε. Here R_i are the horizontally oriented dynamic integration functions,

$$R_i(x, y) = \tau_{iz}|_{S_1}\,. \tag{18}$$

2.4 Thin-sheet force balance

Approximate equality in (13), the first major (dynamic) simplification of our thin-sheet treatment, results in inaccurate profiles of pressure and vertical shear stresses (marked by primes). To compensate for this error, the inaccurate profiles of stresses (eqs 13 and 17) need correction to satisfy the complete (non-truncated) integrated force equilibrium eqs (7) and (8) (after subtraction of eq. 16) following the 'thin-sheet force balance' form:

$$-\frac{\partial \overline{P'}}{\partial x_i} + \frac{\partial\, \overline{\tau_{ij}}}{\partial x_j} + \overline{T_i'} = 0\,, \tag{19}$$

$$\frac{\partial \overline{\tau'_{jz}}}{\partial x_j} + \overline{T'_z} = 0\,, \tag{20}$$

and to satisfy eq. (12) (the depth integration of vertical shear stress):

$$\overline{\tau'_{iz}} = \overline{z_c T'_j} + \left[\frac{-\partial \overline{z_c \cdot P'}}{\partial x_i} + \frac{\partial \overline{z_c \cdot \tau_{ij}}}{\partial x_j} - \overline{P'}\, \frac{\partial w}{\partial x_i} + \overline{\tau_{ij}}\, \frac{\partial w}{\partial x_j} \right], \tag{21}$$

where $(\overline{T'_x}, \overline{T'_y}, \overline{T'_z})$ is a vector related to the sum of the boundary tractions acting on the upper surface ($z=S_2$) and the base ($z=S_1$):

$$\begin{aligned}
&\overline{T'_i}=\left((-P'+\tau_{ij})\,\frac{\partial S_2}{\partial x_j}+\tau'_{iz}\right)\Big|_{S_2}-\left((-P'+\tau_{ij})\,\frac{\partial S_1}{\partial x_j}+\tau'_{iz}\right)\Big|_{S_1},\\
&\overline{T'_z}=-\tau'_{jz}|_{S_2}\cdot\frac{\partial S_2}{\partial x_j}+\tau'_{jz}|_{S_1}\cdot\frac{\partial S_1}{\partial x_j}
\end{aligned}\tag{22}$$

and

$$\overline{(z_c T'_i)}=\left(z_c(-P+\tau_{ij})\,\frac{\partial S_1}{\partial x_j}+z_c\tau_{iz}\right)\Big|_{S_1}+\left(z_c(-P+\tau_{ij})\,\frac{\partial S_2}{\partial x_j}+z_c\tau_{iz}\right)\Big|_{S_2}.\tag{23}$$

Note that, due to the simplification in (13), we cannot claim direct equality of primed tractions (eq. 22) with full boundary tractions (eq. 10), and their relation requires additional investigation (see below). According to eq. (13), depth averaging of pressure yields

$$\overline{P'}=-R_z H-\overline{\tau_{jj}}-\overline{\overline{\rho}}\,.\tag{24}$$

Similarly, the moment of pressure is

$$\overline{z_c\cdot P'}=-\overline{M_\rho}-R_z\overline{z_c}-\overline{z_c\cdot\tau_{jj}}\,.\tag{25}$$

Substitution of eqs (21), (24) and (25) into eqs (19) and (20) yields the final form of the 'thin-sheet force balance equations':

$$\frac{\partial\overline{\tau_{ij}}}{\partial x_j}+\frac{\partial\overline{\tau_{ij}}}{\partial x_i}+\frac{\partial}{\partial x_i}(R_z H+\overline{\overline{\rho}})+\overline{T'_i}=0\,,\tag{26}$$

$$\frac{\partial^2\overline{z_c\cdot\tau_{kj}}}{\partial x_k\partial x_j}+\frac{\partial^2}{\partial x_j\partial x_j}[\overline{z_c\cdot\tau_{kk}}+\overline{M_\rho}+R_z\overline{z_c}]+\frac{\partial}{\partial x_j}\left[(R_z H+\overline{\overline{\rho}}+\overline{\tau_{kk}})\,\frac{\partial w}{\partial x_j}+\overline{\tau_{kj}}\,\frac{\partial w}{\partial x_k}\right]+\frac{\partial}{\partial x_j}(\overline{z_c T'_j})+\overline{T'_z}=0\,.\tag{27}$$

These equations represent corrections for low-order asymptotic approximations (eqs 13 and 17) by the condition of the exact integrated equilibrium (eqs 6 and 7). Therefore, eqs (26) and (27) represent a high-order asymptotic approach of the model presented here.

Let us consider the relations between inaccurate (primed) and accurate (full) boundary tractions. According to the assumption of integrated equality of the inexact and exact solutions, for terms related to boundary tractions in eqs (26), (27) can be written as

$$\begin{aligned}
&\overline{T_i}=\overline{T'_i},\qquad \overline{z_c T_i}=\overline{z_c T'_i},\\
&\overline{T_z}=\overline{\rho}+\varepsilon^2\overline{T'_z}\,.
\end{aligned}\tag{28}$$

Therefore, the horizontal projection of relations between internal and external boundary stresses can be specified via dynamic integration functions and horizontal stresses using

$$\begin{aligned}
&T_i|_{S_1}=-R_i+(R_z+\tau_{jj})\,\frac{\partial S_1}{\partial x_i}+\tau_{ij}\,\frac{\partial S_1}{\partial x_j}\,,\\
&T_i|_{S_2}=\overline{T_i}-T_i|_{S_1}\,.
\end{aligned}\tag{29}$$

The relation between the vertical tractions in eq. (28) represent the correction of the lithostatic condition in eq. (16) to the sum of the full boundary tractions. The separation of this integrated condition cannot be performed in the same way as in the horizontal separation (eq. 29) because the vertical boundary stress relation is described by only a single equation in eqs (28). Therefore, the separation is performed by introducing the partitioning coefficient a_z:

$$T'_z|_{S_1}=(1-a_z)\overline{T'_z},\qquad T'_z|_{S_2}=a_z\overline{T'_z}\,.\tag{30}$$

The full vertical boundary tractions can now be expressed via the vertical dynamic function and partitioning coefficient a_z. Using eqs (13), (16) and (28),

$$\begin{aligned}
&T_z|_{S_1}=-R_z-\varepsilon^2(a_z-1)\overline{T'_z}\,,\\
&T_z|_{S_2}=R_z+\overline{\rho}+\varepsilon^2 a_z\overline{T'_z}\,.
\end{aligned}\tag{31}$$

The partitioning in eqs (30) can be illustrated by the following examples. If $a_z=1$, the bottom boundary condition is satisfied completely by an inexact pressure profile (eq. 13) and $T'_z|_{S_1}=0$. On the other hand, it becomes impossible to satisfy the upper boundary condition using inexact profiles and $\overline{T'_z}=T'_z|_{S_2}$. Setting $a_z=0$ leads to $T'_z|_{S_2}=0$, which satisfies the upper vertical boundary condition by approximate profiles (eqs 13 and 17). Note that, in the case of a stress-free upper surface, R_z represents the sum of the lithostatic pressure with a minus sign and small variations ($\sim\varepsilon^2$) due to the partitioning coefficient.

Summarizing these examples, the setting of the partitioning coefficient to 0 or 1 completely satisfies the upper or bottom vertical boundary condition, respectively, by the simplified profiles expressed by eqs (13) and (17). Values of the partitioning coefficient between 0 and 1 imply satisfying of the boundary condition to different degrees by approximate stress profiles. Note that there is no restriction on the partitioning coefficient being negative or larger than 1, since the main need to satisfy the boundary conditions is accomplished on the basis of two approximation levels, independent of partitioning.

The partitioning coefficient, a_z, represents the degree of freedom in the level of generality applied in this work. It is not clear which boundary condition should have preference in partitioning of the general case. Hence this coefficient should be defined for problems with particular geometry, rheology and boundary conditions.

3 RHEOLOGY-DEPENDENT FORMULATION

3.1 Depth profiles of velocities

Creep rheology assumes that the deviatoric part of the stress tensor depends on the strain rates via viscosity. The viscosity function $\mu=\mu(x, y, z)$ is not assumed to be constant here and can depend on a number of variables:

$$\tau_{ij}=\mu\left(\frac{\partial v_i}{\partial x_j}+\frac{\partial v_j}{\partial x_i}\right), \qquad \tau_{zz}=2\mu\frac{\partial v_z}{\partial z}, \qquad \varepsilon^2\cdot\tau_{iz}=\mu\left(\varepsilon^2\cdot\frac{\partial v_z}{\partial x_i}+\frac{\partial v_i}{\partial z}\right). \tag{32}$$

The creep rheology and incompressibility constrain the depth profiles of the velocities:

$$\begin{aligned}\frac{\partial v_i}{\partial z}&=\varepsilon^2\cdot\left(\frac{\tau_{iz}}{\mu}-\frac{\partial v_z}{\partial x_i}\right),\\ \frac{\partial v_z}{\partial z}&=-\frac{\partial v_i}{\partial x_i}.\end{aligned} \tag{33}$$

Depth integration yields

$$v_i=V_i+\varepsilon^2 R_i\cdot\int_{S_1}^{z}\frac{1}{\mu}\,dz'-\varepsilon^2\int_{S_1}^{z}\frac{\partial v_z}{\partial x_i}\,dz'+q_i. \tag{34}$$

The set of new variables involved in eq. (34), V_i and V_z are the set of kinematic integration functions,

$$\begin{aligned}V_i(x, y)&=v_i(x, y, S_1(x, y)),\\ V_z(x, y)&=v_z(x, y, S_1(x, y))\end{aligned} \tag{35}$$

and

$$q_i=\varepsilon^2\cdot\int_{S_1}^{z}\left(\frac{1}{\mu}\int_{S_1}^{z'}\left(\frac{\partial P}{\partial x_i}-\frac{\partial\tau_{ij}}{\partial x_j}\right)dz''\right)dz'. \tag{36}$$

Note that while the stresses are the same order of magnitude throughout the thin sheet, the velocity and viscosity may have large variations. Therefore, the ε^2 terms are kept, but eq. (36) is reduced to

$$q_i\approx-\varepsilon^2\cdot\int_{S_1}^{z}\left(\frac{1}{\mu}\int_{S_1}^{z'}\frac{\partial}{\partial x_i}\left(\int_{S_1}^{z''}\rho\,dz'''\right)dz''\right)dz'-\varepsilon^2\cdot\int_{S_1}^{z}\frac{(z'-S_1)}{\mu}\,dz'\cdot\frac{\partial R_z}{\partial x_i}-\varepsilon^2\cdot\int_{S_1}^{z}\left(\frac{1}{\mu}\int_{S_1}^{z'}\left(\frac{\partial}{\partial x_k}(2\mu e_{ik})+\frac{\partial}{\partial x_i}(2\mu e_{kk})\right)dz''\right)dz', \tag{37}$$

where P is eliminated using eq. (13), and

$$e_{ij}=\frac{1}{2}\left(\frac{\partial V_i}{\partial x_j}+\frac{\partial V_j}{\partial x_i}\right), \tag{38}$$

where e_{ij} is the basal plane strain rate related to the horizontal velocity components applied on the boundary S_1. From the incompressibility constraint,

$$\begin{aligned}\int_{S_1}^{z}\frac{\partial v_z}{\partial x_i}\,dz'&=\frac{\partial V_z}{\partial x_i}(z-S_1)-\int_{S_1}^{z}\left(\frac{\partial}{\partial x_i}\int_{S_1}^{z'}\frac{\partial v_j}{\partial x_j}\,dz''\right)dz'\\ &\approx\frac{\partial V_z}{\partial x_i}(z-S_1)-\int_{S_1}^{z}\left(\frac{\partial}{\partial x_i}\int_{S_1}^{z'}\tilde{e}_{jj}\,dz''\right)dz',\end{aligned} \tag{39}$$

where

$$\tilde{e}_{ij} = e_{ij} + \frac{\varepsilon^2}{2}\left[\frac{\partial}{\partial x_j}\left(\int_{S_1}^{z} \frac{dz'}{\mu}\cdot R_i\right) + \frac{\partial}{\partial x_i}\left(\int_{S_1}^{z} \frac{dz'}{\mu}\cdot R_j\right)\right] \tag{40}$$

is the partly 'corrected' e_{ij}. Medvedev & Podladchikov (1999) conducted systematic experiments to check the robustness of these approximations. The τ_{ij} component of the stress tensor is related to velocity by

$$\tau_{ij} = \mu\left(\frac{\partial v_i}{\partial x_j} + \frac{\partial v_j}{\partial x_i}\right)$$

$$= \mu\frac{\partial}{\partial x_j}\left(V_i + \varepsilon\cdot\int_{S_1}^{z}\frac{1}{\mu}\,dz'\cdot R_i - \varepsilon^2\int_{S_1}^{z}\frac{\partial v_z}{\partial x_i}\,dz' + q_i\right) + \mu\frac{\partial}{\partial x_i}\left(V_j + \varepsilon\cdot\int_{S_1}^{z}\frac{1}{\mu}\,dz'\cdot R_j - \varepsilon^2\int_{S_1}^{z}\frac{\partial v_z}{\partial x_j}\,dz' + q_j\right). \tag{41}$$

Using eqs (37) and (39) as simplifying assumptions and eqs (38) and (40) for the notation convention, eq. (41) can be rewritten as

$$\tau_{ij} = 2\mu e_{ij} - \varepsilon^2\mu\left[\frac{\partial}{\partial x_j}\left(\frac{\partial V_z}{\partial x_i}(z-S_1)\right) + \frac{\partial}{\partial x_i}\left(\frac{\partial V_z}{\partial x_j}(z-S_1)\right) - \frac{\partial}{\partial x_j}\left(\int_{S_1}^{z}\left(\frac{1}{\mu}\int_{S_1}^{z'}\left(\frac{\partial}{\partial x_k}(2\mu e_{ik}) + \frac{\partial}{\partial x_i}(2\mu e_{kk})\right)dz''\right)dz'\right)\right.$$

$$- \frac{\partial}{\partial x_i}\left(\int_{S_1}^{z}\left(\frac{1}{\mu}\int_{S_1}^{z'}\left(\frac{\partial}{\partial x_k}(2\mu e_{jk}) + \frac{\partial}{\partial x_j}(2\mu e_{kk})\right)dz''\right)dz'\right) + \frac{\partial}{\partial x_j}\left(\int_{S_1}^{z}\left(\frac{\partial}{\partial x_i}\int_{S_1}^{z'}\tilde{e}_{kk}dz''\right)dz'\right) + \frac{\partial}{\partial x_i}\left(\int_{S_1}^{z}\left(\frac{\partial}{\partial x_j}\int_{S_1}^{z'}\tilde{e}_{kk}dz''\right)dz'\right)$$

$$+ \frac{\partial}{\partial x_j}\left(\int_{S_1}^{z}\frac{1}{\mu}\,dz'\cdot R_i\right) + \frac{\partial}{\partial x_i}\left(\int_{S_1}^{z}\frac{1}{\mu}\,dz'\cdot R_j\right) - \frac{\partial}{\partial x_j}\left(\int_{S_1}^{z}\frac{(z'-S_1)}{\mu}\,dz'\cdot\frac{\partial R_z}{\partial x_i}\right) + \frac{\partial}{\partial x_i}\left(\int_{S_1}^{z}\frac{(z'-S_1)}{\mu}\,dz'\cdot\frac{\partial R_z}{\partial x_j}\right)$$

$$\left. - \frac{\partial}{\partial x_j}\left(\int_{S_1}^{z}\left(\frac{1}{\mu}\int_{S_1}^{z'}\frac{\partial}{\partial x_i}\left(\int_{S_1}^{z''}\rho dz'''\right)dz''\right)dz'\right) - \frac{\partial}{\partial x_i}\left(\int_{S_1}^{z}\left(\frac{1}{\mu}\int_{S_1}^{z'}\frac{\partial}{\partial x_j}\left(\int_{S_1}^{z''}\rho dz'''\right)dz''\right)dz'\right)\right]. \tag{42}$$

Finally, the expression for horizontal stresses can be given in a form in which each term is presented by the multiplication of a 'coefficient' (which depends on the geometry, rheology, density distributions and all coordinates) and a 'key unknown function' (a kinematic or dynamic integration function, which is independent of depth):

$$\tau_{ij} = 2\mu e_{ij} - 2J_*\frac{\partial^2 V_z}{\partial x_i\partial x_j} + J_j\frac{\partial V_z}{\partial x_i} + J_i\frac{\partial V_z}{\partial x_j} - 2G_{jk}e_{ik} - 2G_{*k}\frac{\partial e_{ik}}{\partial x_j} - 2G_{j*}\frac{\partial e_{ik}}{\partial x_k} - 2G_{**}\frac{\partial^2 e_{ik}}{\partial x_j\partial x_k}$$

$$- 2G_{ik}e_{jk} - 2G_{*k}\frac{\partial e_{jk}}{\partial x_i} - 2G_{*i}\frac{\partial e_{jk}}{\partial x_k} - 2G_{**}\frac{\partial^2 e_{jk}}{\partial x_i\partial x_k} + 2(F_{ij} - G_{ji} - G_{ji})e_{kk} + 2(F_{i*} - G_{*i} - G_{i*})\frac{\partial e_{kk}}{\partial x_j}$$

$$+ 2(F_{j*} - G_{*j} - G_{j*})\frac{\partial e_{kk}}{\partial x_i} + 2(F_{**} - 2G_{**})\frac{\partial^2 e_{kk}}{\partial x_i\partial x_j} + D_*\left(\frac{\partial R_i}{\partial x_j} + \frac{\partial R_j}{\partial x_i}\right) + D_iR_j + D_jR_i$$

$$- 2\tilde{D}_{***}\frac{\partial^3 R_k}{\partial x_i\partial x_j\partial x_k} - 2\tilde{D}_{i**}\frac{\partial^2 R_k}{\partial x_j\partial x_k} - 2\tilde{D}_{j**}\frac{\partial^2 R_k}{\partial x_i\partial x_k} - 2\tilde{D}_{**k}\frac{\partial^2 R_k}{\partial x_i\partial x_j} - 2\tilde{D}_{i*k}\frac{\partial R_k}{\partial x_j} - 2\tilde{D}_{j*k}\frac{\partial R_k}{\partial x_i} - (\tilde{D}_{ij*} + \tilde{D}_{ji*})\frac{\partial R_k}{\partial x_k}$$

$$- (\tilde{D}_{ijk} + \tilde{D}_{jik})R_k - 2E_*\frac{\partial^2 R_z}{\partial x_i\partial x_j} - E_i\frac{\partial R_z}{\partial x_j} - E_j\frac{\partial R_z}{\partial x_i} - Q_{ij} - Q_{ji}\,. \tag{43}$$

Here the coefficients are

$$
\begin{aligned}
D_i &= \varepsilon^2 \cdot \mu \frac{\partial}{\partial x_i}\left(\int_{S_1}^{z} \frac{1}{\mu}\, dz'\right),\\
\tilde{D}_{ijk} &= \varepsilon^4 \cdot \mu \frac{\partial}{\partial x_i}\left(\int_{S_1}^{z}\left(\frac{\partial}{\partial x_j}\int_{S_1}^{z'} \frac{\partial}{\partial x_k}\left(\int_{S_1}^{z''} \frac{1}{\mu}\, dz'''\right)dz''\right)dz'\right),\\
E_i &= \varepsilon^2 \cdot \mu \frac{\partial}{\partial x_i}\left(\int_{S_1}^{z} \frac{(z'-S_1)}{\mu}\, dz'\right),\\
F_{ij} &= \varepsilon^2 \cdot \mu \frac{\partial^2}{\partial x_i \partial x_i}\left(\frac{(z-S_1)^2}{2}\right),\\
G_{ij} &= \varepsilon^2 \cdot \mu \frac{\partial}{\partial x_i}\left(\int_{S_1}^{z}\left(\frac{1}{\mu}\int_{S_1}^{z'} \frac{\partial \mu}{\partial x_j}\, dz''\right)dz'\right),\\
J_i &= \varepsilon^2 \cdot \mu \frac{\partial}{\partial x_i}(z-S_1),\\
Q_{ij} &= \varepsilon^2 \cdot \mu \frac{\partial}{\partial x_i}\left(\int_{S_1}^{z}\left(\frac{1}{\mu}\int_{S_1}^{z'} \frac{\partial}{\partial x_j}\left(\int_{S_1}^{z''} \rho dz'''\right)dz''\right)dz'\right).
\end{aligned}
\tag{44}
$$

Each index in these coefficients refers to differentiation with respect to the horizontal coordinate with the same index. The remaining coefficients in eq. (43) can be obtained by skipping the differentiation operator corresponding to the 'star' index position, e.g.

$$
G_{*j} = \varepsilon^2 \mu \cdot \int_{S_1}^{z}\left(\frac{1}{\mu}\int_{S_1}^{z'} \frac{\partial \mu}{\partial x_j}\, dz''\right)dz'. \tag{45}
$$

Note that the position of the 'star' index is insignificant in the evaluation of coefficients $\tilde{D}$ and F and significant only for G. For all j and k,

$$
\tilde{D}_{*jk} = \tilde{D}_{j*k} = \tilde{D}_{jk*}, \quad \tilde{D}_{**k} = \tilde{D}_{*k*} = \tilde{D}_{k**}, \quad F_{*j} = F_{j*}, \quad G_{*j} \neq G_{j*}. \tag{46}
$$

Eqs (43) and (44) play a significant role in the force balance treatment presented by eqs (26) and (27), hence the meaning of each type of term has to be explained.

The term μe_{ij} represents the lowermost level of approximation and is the term common to all thin-sheet models. It refers to the boundary velocity in the SS approach, to an independence of velocity on depth in the PS approach, and is treated as a horizontal force component in the FP approach. The terms G represent different influences of horizontal gradients in the boundary velocity on stress due to vertical variations of viscosity (via eqs 37 and 40). The influence of interaction between vertical and horizontal velocities via incompressibility (eqs 33, 34, 39 and 40) is represented by F related terms. Terms related to coefficients J represent the horizontal gradient in the vertical velocity in the expression for shear stress (eq. 33). The terms G, F and J are significant when dynamic boundary conditions are used in particular problems with velocities as unknowns. High-order derivatives of velocity allow realistic solutions even for short wavelengths in this kind of problem.

The terms D represent the influence of basal shear stresses R_i on variations in velocity (eq. 34). $\tilde{D}$ terms indicate the correction of the strain rate along the basal plane for kinematic functions (eq. 40). The necessity of $\tilde{D}$ terms can be illustrated by setting the velocity on the bottom boundary to zero. In this case the vertical velocity would not affect the stress balance if $\tilde{D}$ terms are neglected.

Terms E and Q represent different degrees of the influence of gravity on depth variations of the horizontal stresses due to vertical stratification of the rheology. E terms refer to the interaction of averaged lithostatic pressure and vertical stratification of viscosity. Q terms represent corrections of E terms due to density variations (eqs 36 and 37).

Previously, only the terms μe_{ij} (in the SS, PS and FP approaches), DR_i (in the SS approach) and JV_z (in the FP approach) were employed in thin-sheet approximations. All the other terms represent second- and third-order approximations with respect to ε. However, including them allows more realistic solutions because they can play a significant role in balancing forces.

The coefficients (44) illustrate the assumption about the dependence of viscosity on all coordinates since they involve the derivatives of viscosity with respect to the horizontal coordinates and integration with respect to the vertical coordinate. Possible non-linearity in creep rheology (e.g. power law creep) can be resolved by iterations during numerical calculations without additional analytical investigations.

Horizontal stresses are presented in the form of eq. (43) to simplify the averaging of horizontal stresses and their moments in the thin-sheet force balance in eqs (26) and (27). The form presented in eq. (43) allows averaging by the integration of only the coefficients in eqs (44) (for averaged stresses) or by integrating these coefficients multiplied by a centred vertical coordinate z_c (for averaged moments).

The equations of this section were checked using Maple codes created for symbolic derivations on a computer.

3.2 Closed system of equations for a thin sheet

The system of eqs (26) and (27) together with the expression for the horizontal components of the stress tensor (eq. 43) and the boundary conditions in eqs (29) and (31) represent the closed system of equations for our extended thin-sheet approximation. There are three 'key' unknown functions for each dimension. This results in nine key unknown functions of (x, y) in total:

$$\begin{aligned}
&\text{(a) kinematic:} \quad V_x(x,y) \quad V_y(x,y) \quad V_z(x,y)\,;\\
&\text{(b) dynamic:} \quad R_x(x,y) \quad R_y(x,y) \quad R_z(x,y)\,;\\
&\text{(c) dynamic:} \quad \overline{T_x}(x,y) \quad \overline{T_y}(x,y) \quad \overline{T_z'}(x,y)\,.
\end{aligned} \tag{47}$$

Therefore, at our chosen level of approximation, we can satisfy two boundary conditions on the horizontal boundaries (i.e. all required) and the depth-averaged force balance, eqs (26)–(27). These three conditions in each direction close the system.

The horizontal derivatives remaining in eqs (26)–(27) allow the depth-averaged lateral boundary conditions to be satisfied.

3.3 Operator form of extended thin-sheet approximation equations

After substitution of the horizontal stresses eq. (43), the system of eqs (26)–(27) can be written in operator form:

$$\begin{aligned}
&\mathbf{L}^4_{ij}[V_j]+\mathbf{L}^3_{iz}[V_z]+\tilde{\mathbf{L}}^4_{ij}[R_j]+\tilde{\mathbf{L}}^3_{iz}[R_z]+\overline{T_i}=\mathbf{\Phi}_i(x,y)\,,\\
&\mathbf{L}^5_{zj}[V_j]+\mathbf{L}^4_{zz}[V_z]+\tilde{\mathbf{L}}^5_{zj}[R_j]+\tilde{\mathbf{L}}^4_{zz}[R_z]+\frac{\partial}{\partial x_j}\left(\overline{z_c T_j}\right)+\overline{T_z'}=\mathbf{\Phi}_z(x,y)\,.
\end{aligned} \tag{48}$$

The remaining key dynamic functions in eq. (47) can be reconstructed via the partitioning of eqs (28)–(31). The right-hand function $\mathbf{\Phi}$ does not depend on any key function. The $\mathbf{L}^n$ is the differential operator of order n and is linear with respect to its argument indicated in square brackets. These operators can be described (for $\{r, t\}=\{x, y, z\}$) as

$$\begin{aligned}
&\mathbf{L}^n_{rt}=\sum_{k=1}^{n}\sum_{l=1}^{k} a_{rtkl}(x,y)\,\frac{\partial^k}{\partial x^l \partial y^{(k-l)}}\,,\\
&\tilde{\mathbf{L}}^n_{rt}=\sum_{k=0}^{n}\sum_{l=1}^{k} b_{rtkl}(x,y)\,\frac{\partial^k}{\partial x^l \partial y^{(k-l)}}\,.
\end{aligned} \tag{49}$$

Here coefficients a and b can be evaluated via substitution of expressions (43) and (44) into the thin-sheet system of eqs (26)–(27) for plane stress components and collecting relevant terms, e.g.

$$a_{xx44}=-16\overline{G_{**}}+4\overline{F_{**}}, \qquad b_{xx44}=-4\overline{\tilde{D}_{***}}\,. \tag{50}$$

The system of eqs (48) can be completed by kinematic conditions such as changes in horizontal and vertical velocities across the whole thickness of the sheet (from eqs 34 and 2), which in operator form are

$$\begin{aligned}
&v_i|^{S_2}_{S_1}=\mathbf{M}^2_{ij}[V_j]+\mathbf{M}^1_{iz}[V_z]+\tilde{\mathbf{M}}^2_{ij}[R_j]+\tilde{\mathbf{M}}^1_{iz}[R_z]+\mathbf{\Phi}_{ki}(x,y)\,,\\
&v_z|^{S_2}_{S_1}=\mathbf{M}^3_{zj}[V_j]+\mathbf{M}^2_{zz}[V_z]+\tilde{\mathbf{M}}^3_{zj}[R_j]+\tilde{\mathbf{M}}^2_{zz}[R_z]+\mathbf{\Phi}_{kz}(x,y)\,,
\end{aligned} \tag{51}$$

where the operators $\mathbf{M}$ have a similar form to $\mathbf{L}$ in eq. (49) but different coefficients (from eqs 34 and 2).

3.4 Simplified case of a well-stratified lithosphere

The system (26), (27) and (43) can be simplified for the case of the well-stratified lithosphere, a situation common in geodynamical applications involving gravity. Compared to our previous treatment this case is characterized by lateral gradients of density and viscosity that are so low that they can be neglected, together with variations in the position of the basement S_1. These simplifications result in the disappearance of all coefficients (43)–(44) which contain derivations with respect to horizontal coordinates (i.e. only coefficients which have 'stars' as indices are recognized as significant). The reference level w can be defined as flat so that its horizontal

gradients will fall out of the equations. The system then becomes

$$\frac{\partial\overline{\tau_{ij}}}{\partial x_j}+\frac{\partial\overline{\tau_{jj}}}{\partial x_i}+\frac{\partial}{\partial x_i}\,(R_zH+\overline{\overline{p}})+\overline{T_i}=0\,, \tag{52}$$

$$\frac{\partial^2\overline{z_c\cdot\tau_{kj}}}{\partial x_k\partial x_j}+\frac{\partial^2\overline{z_c\cdot\tau_{kk}}}{\partial x_j\partial x_j}+\frac{\partial^2}{\partial x_j\partial x_j}\,(\overline{M_\rho}+\overline{z_c}R_z)+\frac{\partial}{\partial x_j}\,(\overline{z_c T_j})+\overline{T_z'}=0\,, \tag{53}$$

$$\overline{\tau_{ij}}=2\overline{\mu}e_{ij}-2\overline{G_{**}}\,\frac{\partial}{\partial x_k}\left(\frac{\partial e_{ik}}{\partial x_j}+\frac{\partial e_{jk}}{\partial x_i}\right)+2(\overline{F_{**}}-2\overline{G_{**}})\,\frac{\partial^2 e_{kk}}{\partial x_i\partial x_j}-2\overline{J_*}\,\frac{\partial^2 V_z}{\partial x_i\partial x_j}+\overline{D_*}\left(\frac{\partial R_i}{\partial x_j}+\frac{\partial R_j}{\partial x_i}\right)-2\overline{\tilde{D}_{***}}\,\frac{\partial^3 R_k}{\partial x_i\partial x_j\partial x_k}-2\overline{E_*}\,\frac{\partial^2 R_z}{\partial x_i\partial x_j}\,, \tag{54}$$

$$\overline{z_c\tau_{ij}}=2\overline{z_c\mu}e_{ij}-2\overline{z_cG_{**}}\,\frac{\partial}{\partial x_k}\left(\frac{\partial e_{ik}}{\partial x_j}+\frac{\partial e_{jk}}{\partial x_i}\right)+2(\overline{z_cF_{**}}-2\overline{z_cG_{**}})\,\frac{\partial^2 e_{kk}}{\partial x_i\partial x_j}-2\overline{z_cJ_*}\,\frac{\partial^2 V_z}{\partial x_i\partial x_j}+\overline{z_cD_*}\left(\frac{\partial R_i}{\partial x_j}+\frac{\partial R_j}{\partial x_i}\right)$$
$$-2\overline{z_c\tilde{D}_{***}}\,\frac{\partial^3 R_k}{\partial x_i\partial x_j\partial x_k}-2\overline{z_cE_*}\,\frac{\partial^2 R_z}{\partial x_i\partial x_j}\,. \tag{55}$$

Note that when this simplified system is applied to the 2-D case, it has the same properties as the full system (26), (27) and (43) with respect to the linear analyses presented in Medvedev & Podladchikov (1999).

4 BOUNDARY CONDITIONS: SOME EXAMPLES

Let us consider some examples of possible boundary conditions to illustrate the closed nature of our governing equations.

(a) Applying dynamic boundary conditions to both horizontal boundaries results in a system with dynamic terms as knowns and V_i, V_z as unknowns. The governing system can be represented, analogously to eq. (48), as

$$\begin{aligned}&\mathbf{L}^4_{ij}[V_j]+\mathbf{L}^3_{iz}[V_z]=\mathbf{\Phi}^{(a)}_i(x,y)\,,\\&\mathbf{L}^5_{zj}[V_j]+\mathbf{L}^4_{zz}[V_z]=\mathbf{\Phi}^{(a)}_z(x,y)\,.\end{aligned} \tag{56}$$

Here $\mathbf{\Phi}^{(a)}_i$ includes the influence of known dynamic boundary conditions in addition to the common case $\mathbf{\Phi}_i$ from eq. (48). Note that satisfaction of vertical boundary condition includes the partitioning procedure, therefore $\mathbf{\Phi}^{(a)}_i$ includes its dependence on the partitioning coefficient a_z. The velocity field through the model domain is reconstructed via eq. (34) and the incompressibility constraint after kinematic integration functions (V_i and V_z) are defined by eqs (56). Boundary movements are defined by eqs (3)–(2).

To illustrate the character of eq. (56), we present its simplification. As the following equations are derived only for illustration, most numerical coefficients, indices and summations have been dropped. The influences of rheological and boundary gradients are assumed to be insignificant in this crude investigation. The leading terms in the asymptotic treatment in eq. (56) can be presented by the system

$$\begin{aligned}&\overline{\mu}(\nabla^2(V_x)+3\nabla_x(\mathrm{div}(V)))-\overline{J_*}\nabla^2(\nabla_x(V_z))=\dots\,,\\&\overline{\mu}(\nabla^2(V_y)+3\nabla_y(\mathrm{div}(V)))-\overline{J_*}\nabla^2(\nabla_y(V_z))=\dots\,,\\&4\overline{(z_c\mu)}\nabla^2(\mathrm{div}(V))-\overline{z_cJ_*}\nabla^2(\nabla^2(V_z))=\dots\,,\end{aligned} \tag{57}$$

where

$$\nabla^2=\left(\frac{\partial^2}{\partial x^2}+\frac{\partial^2}{\partial y^2}\right)$$

is the Laplacian operator within the horizontal plane,

$$\mathrm{div}(V)=\left(\frac{\partial V_x}{\partial x}+\frac{\partial V_y}{\partial y}\right)$$

is the divergence operator within the horizontal plane, and $\nabla_x=\partial/\partial x$ is the X projection of the gradient operator. We identify the system of eqs (57) as a PS-like system by analogy with the governing equations of England & McKenzie (1983). Indeed, for a single-layer system with constant viscosity, after ignoring the vertical balance and J_* terms in the horizontal force balance, the first two eqs of (57) become X and Y projections of eq. (17) of England & McKenzie (1983) for a power-law exponent $n=1$ (our notation):

$$\begin{aligned}&\nabla^2(V_x)=-3\nabla_x(\mathrm{div}(V))+\dots\,,\\&\nabla^2(V_y)=-3\nabla_y(\mathrm{div}(V))+\dots\end{aligned} \tag{58}$$

(for details see Medvedev & Podladchikov 1999).

The difference in our treatment is that we include the influence of the vertical velocity V_z. This leads to our three-equation system instead of the two governing equations in the PS model. This difference represents a higher level of approximation because horizontal projections of velocity can vary with depth.

The choice of $w = S_1$ leads to $J_* = (\varepsilon^2 z_c \mu)$. If the X- and Y-related equations from the system of eqs (57) are differentiated with respect to x and y respectively, multiplied by $\overline{(z_c \mu)}$ and subtracted from the vertical balance equation multiplied by $\overline{\mu}$, we then obtain the following equation:

$$[\overline{(z_c \mu)}^2 - \overline{(z_c \cdot \overline{(z_c \mu)})}] \cdot \nabla^2(\nabla^2(V_z)) = \dots , \tag{59}$$

which represents the equation with V_z as an asymptotically leading unknown function. The expression in square brackets illustrates the significance of internal rheological distribution.

Consider deformations in a two-layer system caused by a horizontal stress, σ, which initiates a constant strain rate throughout an unperturbed flowing system. We can consider the total horizontal velocity for the 2-D (x, z) case as $V_x = V_x' - \sigma \cdot x/(4\mu)$, where V_x' is a small perturbation of mean flow. If the lower layer is much less viscous and bounded by a compensation level, eq. (59) can be rewritten after extension by an extra term (referring to variations of averaged viscosity in eqs 57) and after the evaluation of coefficients as

$$\frac{\mu_u h_u^3}{3} \frac{\partial^5 S_2}{\partial^4 x \partial t} + \overline{\sigma} \frac{\partial^2 S_2}{\partial^2 x} = \dots . \tag{60}$$

This represents eq. (6-181) of Turcotte & Schubert (1982) with our notation (index u indicates properties of the upper layer). See Medvedev & Podladchikov (1999) for a detailed derivation.

(b) Mixed boundary conditions set at horizontal boundaries: kinematic boundary conditions on the lower boundary, S_1, and dynamic boundary conditions on the upper boundary, S_2. This case is characterized by setting one dynamic and one kinematic condition for each dimension. This allows the exclusion of one dynamic key function (eq. 47) for each dimension. Velocities V_i and V_y are the prescribed boundary velocities. The system (26)–(27) reconstructs the unknown dynamic key functions and can be written in the form of eq. (48):

$$\begin{aligned} &\tilde{\mathbf{L}}^4_{ij}[R_j] + \tilde{\mathbf{L}}^3_{iz}[R_z] - R_i = \mathbf{\Phi}_i^{(b)}(x, y) , \\ &\tilde{\mathbf{L}}^5_{zj}[R_j] + \tilde{\mathbf{L}}^4_{zz}[R_z] - \frac{\partial}{\partial x_j}((S_1 - w)R_j) - \frac{R_z}{a_z} = \mathbf{\Phi}_z^{(b)}(x, y) . \end{aligned} \tag{61}$$

Here the $\mathbf{\Phi}_i^{(b)}$ include the influence of known kinematic and dynamic boundary conditions in addition to the common case of $\mathbf{\Phi}_i$ from eq. (48). The velocity field through the model domain can be reconstructed via eq. (34) together with the incompressibility constraint after dynamic integration functions (R_i) have been defined by eqs (61). Movements of the boundaries are defined by eqs (3)–(2).

A simplification similar to that performed to obtain eq. (57) allows an illustration of governing equations:

$$\begin{aligned} &-R_x + H\nabla_x(R_z) = -\nabla_x(\overline{\overline{\rho}}) + \dots , \\ &-R_y + H\nabla_y(R_z) = -\nabla_y(\overline{\overline{\rho}}) + \dots , \\ &\overline{(z_c D_*)}\nabla^2(\mathrm{div}(R)) - \frac{1}{a_z}(R_z + \overline{\rho}) = -\nabla^2(\overline{M_\rho}) + \dots , \end{aligned} \tag{62}$$

where the reference surface is chosen as $w = S_1$. This system is similar to that used in the SS approach. The leading terms on the right-hand sides of eqs (62) are written to emphasize the significance of gravity.

We follow Ellis *et al.* (1995) and demonstrate their variation of the SS approach. Consider a system of two layers with constant densities and viscosities subjected to a prescribed horizontal velocity along the base, $V_i(x, y)$. The upper surface is stress free, the upper layer viscosity, μ_u, is much larger than the lower layer viscosity, μ_b. If we assume the velocity profile suggested in the work cited (i.e. the upper layer has a velocity profile independent of depth, $v_i(x, y)$, while the lower layer has a linear (Couette) velocity profile), the horizontal dynamic functions up to the leading asymptotic terms can be written as

$$\begin{aligned} &\overline{T_i} = -R_i = -\frac{\mu_b}{h_b}(v_i - V_i) , \\ &\overline{\tau_{ij}} = 2\overline{\mu} e_{ij} + \overline{D_*}\left(\frac{\partial R_i}{\partial x_j} + \frac{\partial R_j}{\partial x_i}\right) + \dots = \mu_u h_u \left(\frac{\partial v_i}{\partial x_j} + \frac{\partial v_j}{\partial x_i}\right) + \dots . \end{aligned} \tag{63}$$

Here the second equation is obtained by evaluating the coefficients in eq. (43) and neglecting insignificant terms due to the condition $\mu_b \ll \mu_u$. By substituting eqs (63) into eqs (61) and extracting the leading terms, the horizontal force balance in the system

of eqs (62) can be extended, after simplification of the vertical balance ($R_z = -\overline{\rho}$), to

$$2\,\frac{\partial}{\partial x_i}\left(h_{\mathrm{u}}\,\frac{\partial v_i}{\partial x_i}\right)+\frac{\partial}{\partial x_j}\left(h_{\mathrm{u}}\left(\frac{\partial v_i}{\partial x_j}+\frac{\partial v_j}{\partial x_i}\right)\right)-\frac{\mu_{\mathrm{b}}}{h_{\mathrm{b}}\mu_{\mathrm{u}}}\,(v_i-V_i)=\frac{1}{\mu_{\mathrm{u}}}\,\frac{\partial}{\partial x_j}\,(H\overline{\rho}-\overline{\overline{\rho}})\,. \tag{64}$$

This represents eq. (13) of Ellis *et al.* (1995) without corrections due to Airy isostasy on the right-hand side. The full asymptotic analysis of this model is presented in Medvedev & Podladchikov (1999).

The main difference between the two approaches (ETSA and SS) at the level of simplification considered is in the vertical force balance. In contrast to the SS approach, the ETSA recognizes the significance of gradients in vertical force balance. Substitution of the first two eqs of (62) into the vertical balance gives

$$H\overline{(z_{\mathrm{c}}D_*)}\nabla^2(\nabla^2(R_z))-\frac{1}{a_z}\,(R_z+\overline{\rho})=\nabla^2(\overline{\overline{\rho}}-\overline{M_\rho})+\ldots\,. \tag{65}$$

(c) Mixed boundary conditions set at horizontal boundaries: kinematic for tangential X and Y projections, and dynamic boundary conditions for the normal Z projection. This case is characterized by setting two dynamic conditions on the Z direction. This allows the assignment of vertically oriented dynamic key functions using partitioning eqs (28)–(31). Setting two kinematic conditions does not allow the definition of two key functions for each horizontal dimension in eq. (47) because two of them are dynamic and cannot be assigned directly by the kinematic boundary condition. To resolve this problem, the horizontal velocity profile, eq. (51), is treated as a governing equation and should be solved simultaneously with system equations (26)–(27) (not sequentially as in cases a and b). The velocities V_i and V_y are prescribed along the boundary S_1. The total system can be written in operator form:

$$\begin{aligned}
&\mathbf{L}^3_{iz}[V_z]+\tilde{\mathbf{L}}^4_{ij}[R_j]+\overline{T_i}=\mathbf{\Phi}^{(c)}_i(x,y)\,,\\
&\mathbf{L}^4_{zz}[V_z]+\tilde{\mathbf{L}}^5_{zj}[R_j]+\frac{\partial}{\partial x_j}(\overline{z_{\mathrm{c}}T_j})=\mathbf{\Phi}^{(c)}_z(x,y)\,,\\
&\mathbf{M}^1_{iz}[V_z]+\tilde{\mathbf{M}}^2_{ij}[R_i]=\mathbf{\Phi}^{(c)}_{ki}(x,y)\,.
\end{aligned} \tag{66}$$

A simplification similar to that performed to obtain eq. (57) illustrates the character of the governing equations. The kinematic equation in the system of eqs (66) allows the crude assignment of R_i by boundary tractions. The remaining equations can be simplified to

$$\begin{aligned}
&\overline{T_x}+\overline{J_*}\nabla^2(\nabla_x(V_z))=\ldots\,,\\
&\overline{T_y}+\overline{J_*}\nabla^2(\nabla_y(V_z))=\ldots\,,\\
&H\,\mathrm{div}(\overline{T})+\overline{z_{\mathrm{c}}J_*}\nabla^2(\nabla^2(V_z))=\ldots\,,
\end{aligned} \tag{67}$$

The vertical force balance is then in the form of the bending equation. Substitution of the two first equations into the vertical balance gives

$$(\overline{z_{\mathrm{c}}J_*}-H\overline{J_*})\nabla^2(\nabla^2(V_z))=\ldots\,. \tag{68}$$

Ribe (1996) investigated the buoyancy-driven flow of a hot mantle plume (of thickness $S(x)$ and density ρ) bounded by a lithosphere (of thickness $b(x)$ and density ρ) on level $z=-b$, and bounded by a stable asthenosphere (with density ρ_m) on level $z=-(b+S)$. Kinematic boundary conditions assume zero horizontal velocities on both boundaries (top and bottom) of the plume. Neglecting vertical motion of the boundaries renders the crude system of eqs (67) trivial and it is only necessary to specify R_x in this 2-D case. Airy isostasy (the dynamic vertical boundary condition) gives $R_z=\rho_m(L-b-S)$, where $L=$const refers to a lithosphere-free isostatic level in the mantle. Substitution of this condition into the kinematic equation in eqs (66) and ignoring topography gives

$$R_x=\frac{\Delta\rho S}{2}\cdot\frac{\partial}{\partial x}\,(b+S)\,. \tag{69}$$

Substitution of the dynamic integration functions into the velocity profile eq. (34) gives the channel flow in Ribe (1996), expressed as

$$v_x(x,z)=-\frac{\Delta\rho S}{2}\,(z+b+S)(z+b)\,\frac{\partial}{\partial x}\,(b+S)\,, \tag{70}$$

with the difference in sign resulting from us taking the Z-axis in the opposite direction.

(d) Mixed boundary conditions set at horizontal boundaries: dynamic boundary conditions for tangential X and Y projections, and all kinematic boundary conditions set for normal Z projection. This case is characterized by setting dynamic conditions in two horizontal directions, which allows the assignment of horizontally oriented dynamic key functions using eqs (29). Setting two kinematic conditions on the vertical direction requires integration of the incompressibility condition in the form of eq. (51). Velocity

V_z is prescribed along the lower boundary. The governing system to define unknown key functions $V_x(x, y)$, $V_y(x, y)$ and $\overline{T_z^{(1)}}$ is

$$\begin{aligned}
&\mathbf{L}_{ij}^4[V_j]+\mathbf{L}_{iz}^3[R_z]=\mathbf{\Phi}_i^{(d)}(x, y)\,,\\
&\mathbf{L}_{zj}^5[V_j]+\mathbf{L}_{zz}^4[R_z]+\overline{\Delta T_z'}=\mathbf{\Phi}_z^{(d)}(x, y)\,,\\
&\mathbf{M}_{zj}^3[V_j]+\tilde{\mathbf{M}}_{zz}^2[R_z]=\mathbf{\Phi}_k^{(d)}(x, y)\,.
\end{aligned} \tag{71}$$

The simplification equivalent to that leading to eq. (57) shows the type of governing equations. The vertical force balance assigns the function $\overline{T_z^{(1)}}$. The horizontal force balance and kinematic equations (71) can be presented in the form

$$\begin{aligned}
&\overline{\mu}(\nabla^2(V_x)+3\nabla_x(\mathrm{div}(V)))+H\nabla_x(R_z)=-\nabla_x(\overline{\overline{\rho}})+\ldots\,,\\
&\overline{\mu}(\nabla^2(V_y)+3\nabla_y(\mathrm{div}(V)))+H\nabla_y(R_z)=-\nabla_y(\overline{\overline{\rho}})+\ldots\,,\\
&H\,\mathrm{div}(V)+\overline{(E_*\mu^{-1})}\nabla^2(R_z)=-v_z|_{S_1}^{S_2}+\ldots\,.
\end{aligned} \tag{72}$$

This system is similar to the 2-D Stokes system of equations for compressible fluids.

5 DISCUSSION AND CONCLUSIONS

5.1 Complications

The asymptotic treatment presented in this paper results in eqs (26)–(27). After substitution of expressions for the horizontal components of the stress tensor eq. (43) with coefficients (44) the system becomes cumbersome, especially in comparison with the initial equations (5)–(6) and with previous thin-sheet approximations. However, there are several points of note.

First, all kinds of terms in equations were investigated for their necessity. As a result, several insignificant terms were dropped. By comparison, the bending equation (6-189) in Turcotte & Schubert (1982) refers to the fourth-order derivative of vertical velocity with respect to the horizontal coordinate. This is the precise derivative of the vertical force balance eq. (27).

Second, this kind of complexity is usual in the high-order asymptotic description of continua. We can refer to thin elastic plate theory as a close analogue of our investigations based on creep rheology [see Timoshenko & Woinowsky-Krieger (1959) and the recent paper by Van Wees & Cloetingh (1994)].

Third, the long equations do not complicate numerical treatment. For each type of boundary condition, the ETSA results in a system of 2-D equations which can be solved using standard numerical recipes.

Fourth, the applications of the ETSA to particular problems with specific 3-D geometries and rheological properties simplifies the system, as demonstrated by the example discussed in Section 3.4.

5.2 Vertical force balance

This equation is the main complexity discussed in the previous paragraph. However, the vertical force balance in the form of eq. (27) preserves the bending moments and allows realistic behaviour, including a description of the characteristic wavelengths developed by instabilities. This is demonstrated in the accompanying work (Medvedev & Podladchikov 1999) and by previous analyses based on the full equations (e.g. Ramberg 1970a).

The vertical force balance represents the principal difference between the ETSA and previous generations of thin-sheet approximations based on the PS and SS models. The simplest schemes were used mainly to described vertical force balance such as Airy isostasy. The complications of this balance (especially in forms that preserve moments of forces in the equations) were not recognized as significant for the description of creep in thin sheets by most previous authors. This conclusion is correct on the level of generality of previous thin-sheet approximations. However, we present a high-order asymptotic treatment which requires a high-order asymptotic correction to the simple vertical force balance.

Note that preservation of the bending moments was not a target during derivation of the vertical force balance. Depth integration in the form of eq. (12) determines the form of the vertical force balance.

5.3 Free parameters

The present form of the ETSA contains two free parameters: the partitioning coefficient, a_z, and a reference surface for calculating moments, w.

The asymptotic derivation of the ETSA was performed at two levels: the low-level approximation contains the approximate depth profiles of stresses (eqs 13–17), whereas the high level contains the integrated corrections (eqs 27–28). Each level introduces one integration function per dimension (R_i, R_z on the low level, and T_i, T_z on the high level). The relations between these integration functions and boundary tractions are not trivial and require redistribution (partitioning) of exact boundary conditions between the two levels of approximation (eqs 28–31). The analysis showed that the redistribution of vertical projections of boundary tractions can

be performed up to one free parameter, a_z (eq. 30). The value of this partitioning coefficient is related to the degree to which one of the boundary conditions on the low level of approximation is satisfied (see eqs 30 and 31 and the following discussion). Increasing the degree of satisfaction for one boundary condition leads to a decrease of that degree for another boundary. Therefore, the choice of partitioning coefficient represents a preferential choice of one of the boundary conditions. However, it is not obvious which boundary condition should have preference in partitioning in the general case. Hence, this coefficient should be defined for problems with particular geometry, rheology and boundary conditions (see Medvedev & Podladchikov 1999). Note that partitioning of boundary conditions results in small ($\sim\varepsilon^2$) variations in equations and plays a role only if the thin sheet has a highly uneven distribution of mechanical properties (Medvedev & Podladchikov 1999).

The reference surface of stress moments introduced by eq. (12) introduces another degree of freedom in the ETSA. Simple algebra shows that the results of the final system of the thin-sheet force balance (eqs 26–27) are independent of w. However, the choice of the reference surface, w, can change the form of the vertical force balance (eq. 27). The position of the reference surface can be chosen to be appropriate for intended applications of the ETSA.

Analytical investigations require simplification of the equations. The simplest expressions of coefficients resulted from the application of $w=S_1$ (see Medvedev & Podladchikov 1999). This reduces the number of coefficients by a factor of about 2. This simplification becomes even more significant if the basement is considered to be stable ($S_1=\text{const}$).

Another type of simplification is similar to that used in thin elastic plate models (Kooi & Cloetingh 1992). The reference surface is chosen so as to eliminate intraplate stress moments from the bending equation. An application to our model results in the leading terms of X-related key functions vanishing by choosing w so that coefficient $\overline{z_c\mu}$ or $\overline{z_c D}$ is equal to 0. If, in addition, the high-order derivative terms were neglected, the governing system would separate into independent equations. Eq. (26) then describes unknown functions related to the horizontal plane, while eq. (27) defines Z-related unknowns. We did not investigate the details of this kind of simplification, but suspect that it can restrict descriptions of the evolution of instabilities.

For the purpose of numerical treatment, the system of governing equations can be simplified by choosing the position of the reference surface to reduce the singular ($\gg 1$) terms (coefficients). These terms can appear if a viscosity contrast is essential to the study of layered systems.

Another approach is suggested by asymptotic theory (Nayfen 1981) and requires the choice of w by dropping the highest-order derivative of unknown functions in the vertical force balance. After presenting the equations in operator form as eqs (48)–(50), this requires w to be a solution of equations of the type

$$a_{zx5j}=0 \qquad \text{or} \qquad a_{zx5j}=0\,. \tag{73}$$

This simplifies the numerical treatment and makes the asymptotic treatment more balanced.

5.4 Internal stratification

In contrast with previous approaches and full solutions, there is no necessity to specify internal boundary conditions. The continuity of stresses and velocities across internal (rheological) boundaries comes automatically as part of the unified technique presented by the ETSA. This allows a simple description of complicated layered models. The only complication is the evaluation of coefficients (44). Even for the case in which viscosity depends on unknown functions (e.g. power law rheology) the same equations can be investigated numerically by adding iteration procedures.

5.5 Rheology variations

Although creep rheology was applied in this work, other rheologies can be used with the ETSA, but this is beyond the scope of this paper. Applications to a viscoelastic rheology are sketched here merely to demonstrate the potential of the ETSA.

The force balance presented in Section 3 does not depend on rheology, hence changes are required only to the equations in Section 4. Assuming incompressibility, rheological relations eqs (32) can be changed for a Maxwell viscoelastic material to

$$\frac{\tau_{ij}}{\mu}+\frac{1}{\Gamma}\frac{\partial}{\partial t}(\tau_{ij})=\frac{\partial v_i}{\partial x_j}+\frac{\partial v_j}{\partial x_i}\,,\quad \frac{\tau_{zz}}{\mu}+\frac{1}{\Gamma}\frac{\partial}{\partial t}(\tau_{zz})=\frac{\partial v_z}{\partial z}\,,\quad \frac{\tau_{iz}}{\mu}+\frac{1}{\Gamma}\frac{\partial}{\partial t}(\tau_{iz})=\frac{\partial v_z}{\partial x_i}+\varepsilon^{-2}\frac{\partial v_i}{\partial z} \tag{74}$$

(after Turcotte & Schubert 1982) for $\{i, j\}=\{x, y\}$. Here $\Gamma(x, y, z)$ is the elastic shear modulus. The finite difference discretization of time derivatives gives

$$\frac{\partial}{\partial t}(\tau_{kl})=\frac{1}{\Delta t}(\tau_{kl}-\tau_{kl}^{\text{old}})\,. \tag{75}$$

Here τ_{kl}^{old} is the value of stress from the previous time step and Δt is the iteration step. Hence the depth profile of the horizontal velocity, eq. (34), can be corrected for a viscoelastic rheology by changing viscosity, μ, to $\mu_{\text{eff}}=[\mu^{-1}+(\Gamma\Delta t)^{-1}]^{-1}$ and adding an

extra term referring to τ_{kl}^{old}:

$$v_i^{\text{ve}} = v_i^{(34)}|_{\mu\to\mu_{\text{eff}}} - \frac{1}{\Delta t}\int_{s_1}^{z} \frac{\tau_{iz}^{\text{old}}}{\Gamma}\, dz' \,. \tag{76}$$

Here index ve denotes application of the viscoelastic rheology. Changes in the expression for the horizontal stresses, eq. (41), refer to the new definition of horizontal velocities, eq. (76), and the new definition of current stress (from eqs 74 and 75):

$$\tau_{ij}^{\text{ve}} = \mu_{\text{eff}}\left(\frac{\partial v_i^{\text{ve}}}{\partial x_j} + \frac{\partial v_j^{\text{ve}}}{\partial x_i}\right) + \eta_{\text{eff}}\tau_{ij}^{\text{old}} \,, \tag{77}$$

where $\{i, j\} = \{x, y\}$ and $\eta_{\text{eff}} = (1 + \Delta t \cdot \Gamma/\mu)^{-1}$. The corrections of eq. (43) can be described by

$$\tau_{ij}^{\text{ve}} = \tau_{ij}^{(43)}|_{\mu\to\mu_{\text{eff}}} - \frac{\mu_{\text{eff}}}{\Delta t}\left[\frac{\partial}{\partial x_j}\left(\int_{s_1}^{z}\frac{\tau_{iz}^{\text{old}}}{\Gamma}\, dz'\right) + \frac{\partial}{\partial x_i}\left(\int_{s_1}^{z}\frac{\tau_{jz}^{\text{old}}}{\Gamma}\, dz'\right)\right] + \eta_{\text{eff}}\tau_{ij}^{\text{old}} \,. \tag{78}$$

The corrections presented in eqs (76) and (78) refer to the rheological parameter Γ and the stress tensor τ^{old} known from the previous time step. Hence the introduction of this rheology does not require fundamental changes in the general treatment of the ETSA.

5.6 The ETSA versus previous techniques

Existing techniques for modelling 3-D lithospheric structures are direct 3-D numerical treatments and different types of thin-sheet approximations. The results of direct 3-D calculations demonstrate their great potential (e.g. Braun 1993; Braun & Beaumont 1995). However, the very complex numerical techniques and the need for very powerful computing equipment limits this method. The simplicity of the previous generation of thin-sheet approximations allowed simple explanations for a wide variety of lithospheric deformations [England & Jackson (1989), Bird (1989) and Royden (1996) are among a long list of successful applications of thin-sheet models]. However, the simplicity of thin-sheet approximations to date restricts their use.

We have presented a new, extended thin-sheet approximation, with the aim of combining the advantages of existent techniques and broadening their applications. The 2-D system of equations presented here does not increase the systems governing the previous generation of thin-sheet approaches in any fundamental way. On the other hand, the equations developed here can handle all likely boundary conditions and increase the accuracy of applications over a wide range.

The crude derivations of the equations governing previous approaches (Section 4) show that the ETSA represents the general approach and that most previous thin-sheet approaches can be derived by simplifications of our new approach taking account of their specific boundary conditions.

ACKNOWLEDGMENTS

Prof. C. J. Talbot is thanked for initiating and encouraging this work and improving its structure and presentation. The authors thank D. McKenzie, H. Zeyen, A. Poliakov, D. Yuen and two anonymous reviewers for helpful discussions and suggestions that improved the manuscript. This work was supported by an Uppsala University PhD Fellowship to SM.

REFERENCES

Aouvac, J.P. & Burov, E.B., 1996. Erosion as a driving mechanism of intracontinental mountain growth, *J. geophys. Res.,* **101,** 17 747–17 769.

Artyushkov, E.V., 1973. Stress in the lithosphere caused by crustal thickness inhomogeneities, *J. geophys. Res.,* **78,** 7675–7708.

Artyushkov, E.V., 1974. Can the Earth's crust be in a state of isostasy?, *J. geophys. Res.,* **79,** 741–752.

Biot, M.A., 1961, Theory of folding of stratified viscoelastic media and its implications in tectonics and orogenesis, *Geol. Soc. Am. Bull.,* **72,** 1595–1620.

Bird, P., 1989. New finite element techniques for modelling deformation histories of continents with stratified temperature-dependent rheology, *J. geophys. Res.,* **94,** 3967–3990.

Bird, P., 1991. Lateral extrusion of lower crust from under high topography, in the isostatic limit, *J. geophys. Res.,* **96,** 10 275–10 286.

Bird, P. & X. Kong, 1994. Computer simulations of California tectonics confirm very low strength of major faults, *Geol. Soc. Am. Bull.,* **106,** 159–174.

Braun, J., 1993. Three dimensional numerical modeling of compressional orogenies; thrust geometry and oblique convergence, *Geology,* **21,** 153–156.

Braun, J. & Beaumont, C., 1995. Three dimensional numerical experiments of strain partitioning at oblique plate boundaries: implications for contrasting tectonic styles in the southern Coast Ranges, California, and central South Island, New Zealand, *J. geophys. Res.,* **100,** 18 059–18 074.

Buck, W.R., 1991. Modes of continental lithospheric extension, *J. geophys. Res.,* **96,** 20 161–20 178.

Buck, W.R. & Sokoutis, D., 1994. Analogue model of gravitational collapse and surface extension during continental convergence, *Nature,* **369,** 737–740.

Burov, E.B. & Diament, M., 1992. Flexure of the continental lithosphere with multilayered rheology, *Geophys. J. Int.,* **109,** 449–468.

Burov, E.B. & Diament, M., 1995. The effective elastic thickness (T_e) of continental lithosphere: what does it really mean?, *J. geophys. Res.,* **100,** 3905–3927.

Cloetingh, S. & Burov, B., 1996. Thermomechanical structure of European continental lithosphere: constraints from rheological profiles and EET estimates, *Geophys. J. Int.,* **124,** 695–723.

De Bremaecker, J.-C., 1977. Is the oceanic lithosphere elastic or viscous?, *J. geophys. Res.,* **82,** 2001–2004.

Dubois, J., Launay, J., Recy, J. & Marshall, J., 1977. New Hebrides trench: subduction rate from associated lithospheric bulge, *Can. J. Earth Sci.,* **14,** 250–255.

Ellis, S., Fullsack, P. & Beaumont, C., 1995. Oblique convergence of the crust driven by basal forcing: implication for length-scales of deformation and strain partitioning in orogens, *Geophys. J. Int.,* **120,** 24–44.

England, P., 1983. Constraints on extension of continental lithosphere, *J. geophys. Res.,* **88,** 1145–1152.

England, P. & Jackson, J., 1989. Active deformation of the continents, *Ann. Rev. Earth. planet. Sci.,* **17,** 197–226.

England, P. & Houseman, G., 1986. Finite strain calculations of continental deformation, 2, Comparison with the India-Asia collision zone, *J. geophys. Res.,* **91,** 3664–3676.

England, P. & McKenzie, D., 1982. A thin viscous sheet model for continental deformation, *Geophys. J. R. astr. Soc.,* **70,** 295–321.

England, P. & McKenzie, D., 1983. Correction to: a thin viscous sheet model for continental deformation, *Geophys. J. R. Astr. Soc.,* **73,** 523–532.

England, P., Houseman, G. & Sonder, L.J., 1985. Length scales for continental deformations in convergent, divergent, and strike-slip environments: Analytical and approximate solutions for a thin viscous sheet model, *J. geophys. Res.,* **90,** 3551–3557.

Fletcher, R.S., 1977. The shape of single layer folds at small but finite amplitude, *Tectonophysics,* **39,** 593–606.

Fowler, A.C., 1993. Boundary layer theory and subduction, *J. geophys. Res.,* **98,** 21 997–22 005.

Houseman, G. & England, P., 1986. Finite strain calculations of continental deformation. 1. Method and general results for convergent zones, *J. geophys. Res.,* **91,** 3651–3663.

Houseman, G. & England, P., 1993. Crustal thickening versus lateral expulsion in the Indian-Asian continental collision, *J. geophys. Res.,* **98,** 12 233–12 249.

Huppert, H.E., 1982. The propagation of two-dimensional and axisymmetric viscous gravity current over a rigid horizontal surface, *J. Fluid Mech.,* **121,** 43–58.

Huppert, H.E., Shepard, J.B., Sigurtsson, H. & Sparks, R.S.J., 1982. On lava dome growth, with application to the 1979 lava extrusion of the Soufriere of St. Vincent, *J. Volc. Geotherm. Res.,* **14,** 199–222.

Jones, C.H., Unrih, J.R. & Sonder, L.J., 1996. The role of gravitational potential energy in active deformation in the southwestern United States, *Nature,* **381,** 37–41.

Karner, G. & Watts, A.B., 1983. Gravity anomalies and flexure of the lithosphere at mountain ranges, *J. geophys. Res.,* **88,** 10 449–10 477.

Kaufman, P.S. & Royden, L.H., 1994. Lower crustal flow in extensional settings: constraints from the Halloran Hills region, eastern Mojave Desert, California, *J. geophys. Res.,* **99,** 15 723–15 739.

Kooi, H. & Cloetingh, S., 1992. Lithospheric necking and regional isostasy at extensional basins 2. Stress-induced vertical motions and relative sea level changes, *J. geophys. Res.,* **97,** 17 573–17 591.

Lobkovsky, L.I. & Kerchman, V.I., 1991. A two-level concept of plate tectonics: application to geodynamics, *Tectonophysics,* **199,** 343–374.

Lyon-Caen, H. & Molnar, P., 1983. Gravity anomalies of the southern Tibet basin, *Geophys. Res. Lett.,* **11,** 1251–1254.

McKenzie, D., Ford, P.G., Lui, F. & Pettengil, G.H., 1992. Pancake-like domes on Venus, *J. geophys. Res.,* **97,** 15 967–15 976.

McNutt, M., Diament, M. & Kogan, M.G., 1988. Variations of elastic plate thickness at continental thrust belts, *J. geophys. Res.,* **93,** 8825–8838.

Medvedev S.E., 1993. Computer simulation of sedimentary cover evolution, in *Computerized Basin Analysis: the Prognosis of Energy and Mineral Resources,* pp. 1–10, eds Harff, J. & Merriam, D.F., Plenum, New York.

Medvedev S.E. & Podladchikov, Yu.Yu., 1999. New extended thin-sheet approximation for geodynamic applications—II. Two-dimensional examples, *Geophys. J. Int.,* **136,** 586–608 (this issue).

Mikhailov, V.O., Myasnikov, V.P. & Timoshkina, E.P., 1996. Dynamics of the upper cover of the Earth evolution caused by extension or compression, *Phys. Solid Earth*, **6,** 30–37 (in Russian).

Miyamoto, H. & Sasaki, S., 1997. Simulating lava flows by an improved cellular automata method, *Computer Geosci.,* **23,** 183–292.

Myasnikov, V.P., Mikhailov, V.O. & Timoshkina, E.P., 1993. Interaction of mantle and rheologically layered upper cover of the Earth, *Dok. Akad. Nauk, Phys. Solid Earth*, **330,** 771–773 (in Russian).

Nayfen, A.H., 1981. *Introduction to Perturbation Techniques,* Willey, New York.

Ramberg, H., 1970a. Folding of laterally compressed multilayers in the field of gravity, 1, *Phys. Earth planet. Interiors.,* **2,** 203–232.

Ramberg, H., 1970b. Folding of laterally compressed multilayers in the field of gravity, 2, Numerical examples, *Phys. Earth planet. Inter.,* **4,** 83–120.

Ranalli, G., 1994. Nonlinear flexure and equivalent mechanical thickness of the lithosphere, *Tectonophysics,* **240,** 107–114.

Ribe, N.M., 1996. The dynamics of plume-ridge interaction 2. Off-ridge plumes, *J. geophys. Res.,* **101,** 16 195–16 204.

Royden, L., 1996. Coupling and decoupling of crust and mantle in convergent orogens: implications for strain partitioning in the crust, *J. geophys. Res.,* **101,** 17 679–17 705.

Schlichting, G., 1968. *Boundary Layer Theory,* McGraw-Hill, New York.

Sleep, N.H., 1996. Lateral flow of hot plume material ponded at sublithospheric depths, *J. geophys. Res.,* **101,** 28 065–28 083.

Sleep, N.H., 1997. Lateral flow and ponding of starting plume material, *J. geophys. Res.,* **101,** 10 001–10 012.

Smith, R.B., 1975. Unified theory of the onset of folding, boudinage and mullion structure, *Geol. Soc. Am. Bull.,* **86,** 1601–1609.

Sobouti, F. & Arkani-Hamed, J., 1996. Numerical modelling of the deformation of the Iranian Plateau, *Geophys. J. Int.,* **126,** 805–818.

Sonder, L.J. & England, P., 1986. Vertical averages of rheology of the continental lithosphere: relation to thin sheet parameters, *Earth planet. Sci. Lett.,* **77,** 81–90.

Sonder, L.J., England, P. & Houseman, G.A., 1986. Continuum calculations of continental deformation in transcurrent environments, *J. geophys. Res.,* **91,** 4797–4810.

Talbot, C.J., Medvedev, S., Alavi, M., Shahrivar, H. & Heidari, E, 1998. Salt extrusion rates at Kuh-e-Jahani, Iran: June 1994 to November 1996, in preparation.

Timoshenko, S.P. & Woinowsky-Krieger, S., 1959. *Theory of Plates and Shells,* McGraw-Hill, New York.

Turcotte, D.L. & Schubert, G., 1982. *Geodynamics – Applications of Continuum Physics to Geological Problems,* John Willey, New York.

Van Wees, J.D. & Cloetingh, S., 1994. A finite-difference technique to incorporate spatial variations in rigidity and planar faults into 3-D models for lithospheric flexure, *Tectonophysics,* **266,** 343–360.

Vilotte, J.P., Daigniers, M. & Madariaga, R., 1982. Numerical modelling of interplate deformation: simple mechanical models of continental collision, *J. geophys. Res.,* **87,** 10 709–10 728.

Vilotte, J.P., Madariaga, R., Daigniers, M. & Zienkiewicz, O., 1986. Numerical study of continental collision: influence of buoyancy forces and an initial stiff inclusion, *Geophys. J. R. astr. Soc.,* **84,** 279–310.

Westaway, R., 1993. Forces associated with mantle plumes, *Earth planet. Sci. Lett.,* **119,** 331–348.

Zanemonetz, V.B., Kotyolkin, V.D. & Myasnikov, V.P., 1974. The dynamics of lithospheric motion, *Phys. Solid Earth,* **10,** 306–311.

Zanemonetz, V.B., Mikhailov, V.O. & Myasnikov, V.P., 1976. Mechanical model of block folding formation, *Phys. Solid Earth,* **12,** 631–635.